

Mapping color fluctuations in the photon in ultraperipheral heavy ion collisions at the Large Hadron Collider

M. Alvioli,¹ L. Frankfurt,^{2,3} V. Guzey,⁴ M. Strikman,³ and M. Zhalov⁴

¹*Consiglio Nazionale delle Ricerche, Istituto di Ricerca per la*

Protezione Idrogeologica, via Madonna Alta 126, I-06128 Perugia, Italy

²*Nuclear Physics Department, School of Physics and Astronomy, Tel Aviv University, 69978 Tel Aviv, Israel*

³*Department of Physics, the Pennsylvania State University, State College, PA 16802, USA*

⁴*National Research Center “Kurchatov Institute”,*

Petersburg Nuclear Physics Institute (PNPI), Gatchina, 188300, Russia

Using information on photoproduction of light and heavy vector mesons on the nucleon and nuclei, we explicitly model color fluctuations (CFs) in the photon wave function and for the first time make predictions for the distribution over the number of wounded nucleons ν in the inelastic photon–nucleus scattering. We show that CFs lead to a dramatic enhancement of this distribution at $\nu = 1$ and large $\nu > 10$ compared to the standard Glauber model calculations. We also study discuss the implications of CFs in the photon on the total transverse energy ΣE_T and other observables in inelastic γA scattering with different triggers. Our predictions can be tested in proton–nucleus and nucleus–nucleus ultraperipheral collisions at the LHC and will help to map CFs, whose first indications have already been observed at the LHC.

I. INTRODUCTION

The key feature of the high energy strong interactions of energetic composite particles with nuclei is that as a consequence of the uncertainty principle and Lorentz slowing down of the interaction time, the projectile fluctuates into certain configurations, which remain coherent (so-called frozen) during the passage through the nucleus. In pre-QCD times these effects were extensively studied in photon–nucleon (γN) and photon–nucleus (γA) collisions, for a review, see [1]. In QCD this fundamental property of high energy processes, is well understood theoretically and established experimentally, for a review, see, e.g. [2, 3]. In particular it was established that the light vector meson component of the photon wave function is responsible for about 70% of $\sigma_{\text{tot}}(\gamma N)$. The origin of the remaining 30% was a matter of debate.

A distinctive feature of the QCD dynamics, which has been observed in a number of various of experiments, is that the interaction strength of different configurations varies. In particular, as a consequence of color screening, the strength of the interaction of a high energy hadron (photon) in a configuration with a small transverse size is much smaller than the average interaction strength; this phenomenon is called the color transparency in the literature, for a recent review, see [4]. While other mechanisms can also contribute to the fluctuations of the interaction strength of an energetic projectile, we refer to the phenomenon as color fluctuations (CFs).

At collider energies, there have been observed several effects that could be naturally described by CFs. First, the ATLAS study [5] of the dependence of hadron production on the transverse energy ΣE_T in proton–lead (pPb) collisions at $\sqrt{s_{NN}} = 5.02$ TeV showed a significantly broader distribution for negative rapidities $-4.5 < \eta < -3$ than that expected in the geometric Glauber model [6]. This was interpreted in [5] as due to a broader distribution in the number of wounded nucleons. Such broadening naturally emerges in the CF approach [7]. The numerical results of [5] are consistent with the expectations of [8, 9].

The second effect is the observation of a large violation of the Glauber approximation for the dependence of the jet production on the centrality observed in pA collisions at the LHC [10, 11] and in dA collisions at RHIC [12], for which a large- x parton momentum fraction of the proton is involved (a factor of ~ 4 for the ratio of the rates of peripheral and central collisions). At the same time the geometric picture works very well for the collisions with up to eight nucleons, if x is small enough, $x \leq 0.1$. This pattern is consistent with the x -dependent CFs [13].

The third effect is a significant suppression of the rate of ρ meson production in the coherent $\gamma A \rightarrow \rho A$ reaction measured in Pb-Pb ultraperipheral collisions (UPCs) at the LHC [14] as compared to the expectations of the vector dominance model combined with the Glauber approximation for the photon–nucleus interaction. This effect was explained in [15] by taking into account the effect of CFs in the photon, which reduce the effective ρ –nucleon cross section by suppressing the overlap of the vector meson and photon wave functions and lead to sizable inelastic (Gribov) nuclear shadowing due to the photon inelastic diffraction into large masses.

In this paper we argue that one can map the color fluctuations in the photon wave function using ultraperipheral collisions (UPCs) of heavy ions at the LHC. Although feasibility of UPC studies was analyzed at length in [16], the studies discussed below were not addressed. Primarily this is because such analyses became feasible due to the experience accumulated in the analysis of pA collisions at the LHC. In a long run studies along these lines at the

Electron-Ion Collider [17, 18] would provide a detailed information on CFs in the photon and their dependence on the photon virtuality. The main challenge for building a realistic description of the photon–nucleon (nucleus) interactions at collider energies is to take into account the multi-scale structure of the light-cone wave function of the photon associated with presence of soft and hard intrinsic scales. In particular, the photon wave function contains several types of configurations: large- σ configurations characterized by small transverse momenta $k_t < 0.5$ GeV and invariant masses of the order of the mass of light vector mesons interacting with the strength $\sim \sigma_{\pi N}$ ($\sigma_{\pi N}$ is the total pion–nucleon cross section), configurations interacting with σ much larger than $\sigma_{\pi N}$ related to the presence of soft large mass diffraction, and small- σ configurations with large $k_t \geq 1$ GeV, which can interact with several nucleons without additional suppression due to the presence of hard leading twist diffraction, whose contribution results in the leading twist nuclear shadowing.

We propose a unifying model of CFs in the photon by combining the information obtained in the analysis of photoproduction of ρ mesons at the LHC energies [15], which enables us to model the photon configurations interacting mostly with the strength exceeding the typical ρ -nucleon cross section, with that obtained in photoproduction of J/ψ mesons [19], which is amenable to the perturbative QCD (pQCD) description of the weakly interacting configurations. We apply the resulting model of the photon CFs to the calculation of the distribution over the number of wounded nucleons, ν , involved in the inelastic γA scattering. We show that as a consequence of CFs around the average value, the soft inelastic nuclear shadowing effect is strongly enhanced as compared to pA collisions. We also take into account an additional effect of the different pattern of the interaction of small dipoles, which leads to the leading twist nuclear shadowing and which is neglected in the eikonal approximation. This effects leads to significant probability for small dipoles to interact with several nucleons, which noticeably reduces the distribution over ν for small values of ν .

This paper is organized as follows. In Sect. II we develop a model for CFs in the photon for the photon–nucleon interaction. In Sect. III we present and discuss our predictions for the distribution over the number of wounded nucleons (inelastic interactions) in the inelastic photon–nucleus scattering using our model for CFs in the photon without and with an additional effect of the leading twist nuclear shadowing for the configurations interacting with small cross sections. In Sect. IV, we make a prediction for the transverse energy $\sum E_T$ distribution in γA collisions using as a starting point the model of [5] for dependence of $\sum E_T$ on ν . Finally, in Sect. V we discuss possibilities of special triggers, which would allow one to use γA scattering as a fine “strengthnometer” for different components of the photon wave function.

II. THE DISTRIBUTION OVER COLOR FLUCTUATIONS IN THE HIGH-ENERGY PHOTON

At sufficiently high photon energies E_γ in the target rest frame, the coherence length associated with the hadronic fluctuation (component) of the photon of mass M exceeds the target radius R_T , $l_{\text{coh}} = 2E_\gamma/M^2 > R_T$. In this case, the forward photon–target amplitude (the total photoabsorption cross section) can be expressed in terms of the dispersion representation over the masses M^2 [20]:

$$\sigma_{\gamma N} = \frac{\alpha_{\text{e.m.}}}{24\pi^2} \int \frac{dM^2}{M^2} R_{e^+e^- \rightarrow \text{hadrons}}(M^2) \sigma_{MN}, \quad (1)$$

where $\alpha_{\text{e.m.}}$ is the fine structure constant; $R_{e^+e^- \rightarrow \text{hadrons}}(M^2) = \sigma(e^+e^- \rightarrow \text{hadrons})/\sigma(e^+e^- \rightarrow \mu^+\mu^-)$ is the ratio of the e^+e^- annihilation cross sections into hadrons (everything) and a muon pair, respectively, of a given invariant mass squared M^2 ; σ_{MN} is the total cross section for the interaction of a given component with the target. It is important to emphasize that non-diagonal transition between different photon components have been neglected in Eq. (1), which is justified in the case of a heavy nuclear target [20].

In the vector meson dominance model (VMD), 70% of the integral in Eq. (1) is due to the sum of ρ , ω and ϕ mesons, which interact with hadrons with a strength similar to that of a pion (for ρ and ω) [1, 21, 22].

A straightforward generalization of Eq. (1) to the case of deep inelastic scattering (DIS) leads to a gross violation of the approximate Bjorken scaling, which is often called the Gribov paradox in the literature. In the framework of the parton model, the resolution of the Gribov paradox was suggested by Bjorken [23] by assuming that the interaction is dominated by the so-called aligned quark–antiquark pairs, where the quarks share asymmetrically the photon longitudinal momentum and have small transverse momenta p_t . While such configurations correspond to typical vector meson-like interaction cross sections, their contribution to the total virtual photon–nucleon cross section $\sigma_{\gamma^* N}$ is suppressed by a factor of μ^2/M^2 , where μ is a soft QCD scale, which leads to the scaling of $\sigma_{\gamma^* N}$.

In QCD the situation is somewhat different [24]: in addition to the aligned pairs, configurations with large p_t also contribute to $\sigma_{\gamma^* N}$; their noticeable contribution is proportional to $\alpha_s(p_t^2)/p_t^2$, where α_s is the strong coupling constant, and grows with an increase of the collision energy.

Overall this suggests the following approximate picture of the color fluctuations in the photon: the majority of the configurations are similar to the CFs in the $\gamma \rightarrow \rho, \omega$ transitions; they dominate at large and medium $\sigma \geq \sigma_{\pi N}$. (They

also include the fluctuations in the aligned jet component.) Note that with an increase of collision energies, these configurations are likely to be somewhat more localized than those in the elastic vector meson–nucleon scattering [15]. In addition, there is a component which dominates for small σ and which is described by the perturbative (dipole) wave function interacting with the strength given by perturbative QCD.

To quantify CFs, it is convenient to use the formalism of cross section fluctuations [25–28] and to introduce the distribution [29, 30] $P_\gamma(\sigma)$, which gives the probability for the photon to be in a configuration interacting with the nucleon target with the cross section σ . While the form of $P_\gamma(\sigma)$ can be calculated from first principles only for small σ [31], it can be constrained by the following integral relations:

$$\begin{aligned} \int d\sigma P_\gamma(\sigma)\sigma &\equiv \langle\sigma\rangle = \sigma_{\gamma p}, \\ \int d\sigma P_\gamma(\sigma)\sigma^2 &\equiv \langle\sigma^2\rangle = 16\pi \frac{d\sigma_{\gamma p \rightarrow Xp}(t=0)}{dt}, \end{aligned} \quad (2)$$

where $\sigma_{\gamma p}$ is the total photon–nucleon cross section; $d\sigma_{\gamma p \rightarrow Xp}(t=0)/dt$ is the cross section of photon diffractive dissociation on the proton including the ρ meson peak, which determines the dispersion of CFs encoded in $P_\gamma(\sigma)$. Note that the distribution $P_\gamma(\sigma)$ is not normalizable [31], i.e., the integral $\int d\sigma P_\gamma(\sigma)$ is divergent at the lower integration limit due to the infinite renormalization of the photon Green’s function (the vacuum polarization).

Therefore, to model color fluctuations in the photon, we build a model interpolating between the regimes of small and large σ . For the former, we use the color dipole model (CDM) of the photon wave function, where the (usually virtual) photon is treated as superposition of quark–antiquark pairs (dipoles). The dipoles interact with the target with cross sections given by perturbative QCD for small dipoles [32]. Based on the popular assumption that the contribution of light vector mesons to the photon–nucleon cross section is dual to the integral over the masses of $q\bar{q}$ pairs (for example $M^2 \leq 1 \text{ GeV}^2$ for ρ, ω -mesons), we expect that CDM should give a reasonable description of CFs for average $\sigma \sim \sigma(\pi N)$. For large σ , $\sigma \gg \sigma(\pi N)$, the color fluctuations are determined by non-perturbative effects both in terms of the photon configurations involved and the strength of the interaction. Therefore, we use the modified VMD (mVMD) model to model their effect.

In the CDM, the total cross section of photon–proton interaction has the following form:

$$\sigma_{\gamma p}(W) = \sum_q e_q^2 \int dz d^2 d_t \sigma_{q\bar{q}}(W, d_t, m_q) |\Psi_{\gamma, T}(z, d_t, m_q)|^2, \quad (3)$$

where z is the fraction of photon momentum carried by the quark in the dipole; d_t is the transverse distance between the quark and the antiquark; e_q and m_q are the quark charge and mass, respectively; W is the invariant photon–nucleon center of mass energy. The photon wave function squared in the mixed momentum–coordinate representation has the following standard representation [33]:

$$|\Psi_{\gamma, T}(z, d_t, m_q)|^2 = \frac{3\alpha_{\text{e.m.}}}{2\pi^2} [(z^2 + (1-z)^2)\epsilon^2 K_1^2(\epsilon d_t) + m_q^2 K_0^2(\epsilon d_t)], \quad (4)$$

where $\epsilon = m_q$; $K_{0,1}$ are modified Bessel functions of the first kind.

In our analysis we use the results of the CDM developed in [34], which gives a good description of the proton structure function $F_{2p}(x, Q^2)$ down to $Q^2 \sim 0.3 \text{ GeV}^2$. In this approach, the dipole cross section $\sigma_{q\bar{q}}$ is built as a piece-wise form. For small dipoles corresponding approximately to $d_t \leq 0.3 - 0.4 \text{ fm}$, one has

$$\sigma_{q\bar{q}}(W, d_t, m_q) = \frac{\pi^2}{3} d_t^2 \alpha_s(Q_{\text{eff}}^2) x_{\text{eff}} g(x_{\text{eff}}, Q_{\text{eff}}^2), \quad (5)$$

where $Q_{\text{eff}}^2 = \lambda/d_t^2$ for light quarks and $Q_{\text{eff}}^2 = m_q^2 \lambda/d_t^2$ for heavy quarks; $x_{\text{eff}} = 4m_q^2/W^2 + 0.75\lambda/(W^2 d_t^2)$; $m_q = 300 \text{ MeV}$ for light u, d and s quarks and $m_c = 1.5 \text{ GeV}$. This choice of the quark masses ensures that the average transverse size of $q\bar{q}$ configurations in the photon wave function is close to that of the pion, $d_\pi = 0.65 \text{ fm}$, and also leads to a smoother interpolation between small and large σ regimes. The parameter $\lambda = 4$ is chosen to best reproduce the HERA data on diffractive J/ψ photoproduction [35]. Note, however, that heavy quarks give a very small contribution to the quantities we discuss below.

For large dipole sizes, $d_t \geq 0.65 \text{ fm}$, $\sigma_{q\bar{q}}$ is constrained not to exceed the total pion–nucleon cross section at the appropriate energy. Finally, for the intermediate values of $0.3 - 0.4 < d_t < 0.65 \text{ fm}$, $\sigma_{q\bar{q}}$ is modeled as a smooth interpolation between the low- σ (5) and large- σ limits.

Equation (3) can be rewritten in terms of the integral over the cross section $\sigma \equiv \sigma_{q\bar{q}}(W, d_t, m_q)$ (see also [31]):

$$\sigma_{\gamma p}(W) = \int d\sigma \sigma P_\gamma^{\text{dipole}}(\sigma, W), \quad (6)$$

where the probability distribution $P_\gamma(\sigma)$ is:

$$P_\gamma^{\text{dipole}}(\sigma, W) = \sum_q e_q^2 \left| \frac{\pi d d_t^2}{d\sigma_{q\bar{q}}(W, d_t, m_q)} \right| |\Psi_{\gamma,T}(z, d_t, m_q)|^2. \quad (7)$$

The resulting distribution $P_\gamma^{\text{dipole}}(\sigma, W)$ as a function of σ for different light quark masses m_q and at $W = 100$ GeV is shown by the green dashed curves. To examine the sensitivity of $P_\gamma^{\text{dipole}}(\sigma, W)$ to the choice m_q , we varied the light quark mass in the interval $0 \leq m_q < 350$ MeV; the results are shown in Fig. 1, where the upper dashed curve corresponds to $m_q = 0$ and the lower one is for $m_q = 350$ MeV. One sees from the figure that $P_\gamma^{\text{dipole}}(\sigma, W)$ is essentially insensitive to m_q for $\sigma \leq 10$ mb; we take this value of σ as a starting point for the smooth interpolation to the large- σ regime.

Note that since in the dipole model that we use, the dipole cross section does not exceed approximately 40 mb, the resulting distribution $P_\gamma^{\text{dipole}}(\sigma, W)$ of Eq. (7) has support only for $0 \leq \sigma \leq 40$ mb.

For large σ , the distribution $P_\gamma(\sigma)$ can be well approximated by the distribution $P(\sigma)$ for the $\gamma \rightarrow \rho$ transition, which was considered in the framework of the mVMD model [15]. Taking the sum of the ρ , ω and ϕ meson contributions, the resulting distribution reads:

$$P_{(\rho+\omega+\phi)/\gamma}(\sigma, W) = \frac{11}{9} \left(\frac{e}{f_\rho} \right)^2 P(\sigma, W), \quad (8)$$

where $P(\sigma, W)$ is taken from [15]; the coefficient of 11/9 takes into account the ω and ϕ contributions in the SU(3) approximation (which overestimates the rather small contribution of the ϕ mesons). The form of $P(\sigma, W)$ is motivated by $P_\pi(\sigma, W)$ for the pion and takes into account presence of the large-mass diffraction at high energies. It is also constrained to describe the HERA data on ρ photoproduction on the proton, which requires to account for a suppression of the overlap of the photon and ρ wave function as compared to the diagonal case of $\rho \rightarrow \rho$ transition.

The resulting $P_{(\rho+\omega+\phi)/\gamma}(\sigma)$ at $W = 100$ GeV is shown by the blue dot-dashed curve in Fig. 1.

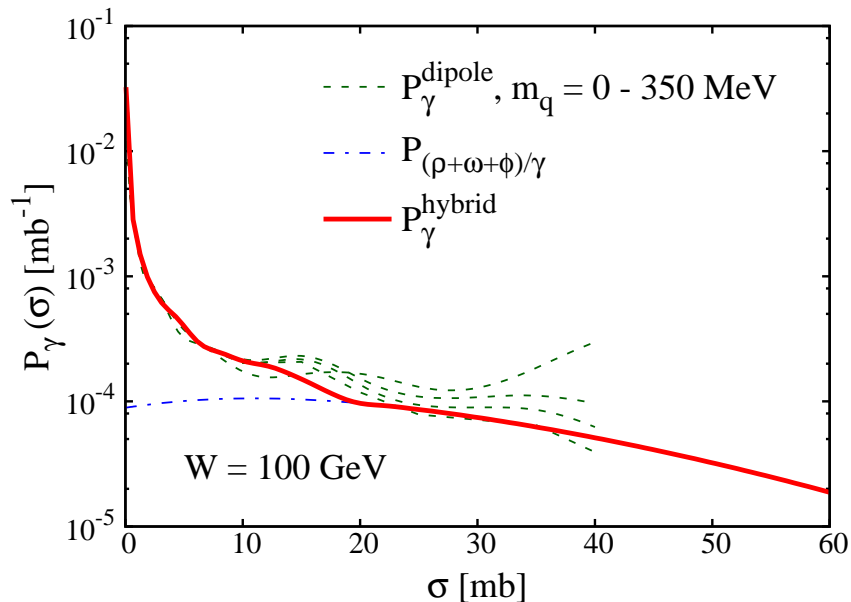


FIG. 1: The distributions $P_\gamma(\sigma)$ for the photon at $W = 100$ GeV. The red solid curve shows the full result of the hybrid model, see Eq. (9). The green dashed and blue dot-dashed curves show separately the dipole model and the vector meson contributions evaluated using Eqs. (7) and (8), respectively.

We build a hybrid model of $P_\gamma(\sigma)$ by interpolating between regimes of small $\sigma \leq 10$ mb, where CDM is applicable and there is no dependence on the light quark mass m_q , and the regime of large σ , where the soft contribution due to the lightest vector meson dominates (hence we neglect the soft contribution of configurations with the large mass and small k_t). In particular, in our analysis we use the following expression:

$$P_\gamma(\sigma) = \begin{cases} P_\gamma^{\text{dipole}}(\sigma), & \sigma \leq 10 \text{ mb}, \\ P_{\text{int}}(\sigma), & 10 \text{ mb} \leq \sigma \leq 20 \text{ mb}, \\ P_{(\rho+\omega+\phi)/\gamma}(\sigma), & \sigma \geq 20 \text{ mb}. \end{cases} \quad (9)$$

where $P_{\text{int}}(\sigma)$ is a smooth interpolating function. The resulting $P_\gamma(\sigma)$ is shown by the red solid curve in Fig. 1.

Our model for $P_\gamma(\sigma)$ satisfies the constraints of Eq. (2) and gives good description of the total and diffraction dissociation photon–proton cross sections at $W = 100$ GeV. Indeed, for $\sigma_{\gamma p}$, we obtain $\int_0^{100 \text{ mb}} d\sigma \sigma P_\gamma(\sigma) = 135 \mu\text{b}$, which with several percent accuracy agrees with the PDG value of $\sigma_{\gamma p} = 146 \mu\text{b}$ [36]. For the cross section of diffractive dissociation, we obtain $\int_0^{100 \text{ mb}} d\sigma \sigma^2 P_\gamma(\sigma)/(16\pi) = 240 \mu\text{b}/\text{GeV}^2$, which agrees with our estimate $d\sigma_{\gamma p \rightarrow X p}(t=0)/dt \approx 220 \mu\text{b}/\text{GeV}^2$, which is obtained by integrating the data of [37] over the produced diffractive masses and extrapolating the resulting cross section to the desired $W = 100$ GeV.

To quantify the width of CFs, one can introduce the dispersion ω_σ . For the photon, it can be introduced by the following relation:

$$\int d\sigma \sigma^2 P_\gamma(\sigma) = (1 + \omega_\sigma) \left(\frac{e}{f_\rho} \hat{\sigma}_{\rho N} \right)^2, \quad (10)$$

where $\hat{\sigma}_{\rho N}$ is the ρ meson–nucleon cross section. The use of our $P_\gamma(\sigma)$ in Eq. (10) gives $\omega_\sigma \approx 0.93$, which should be compared to $\omega_\sigma^\rho \approx 0.54$ for the pure ρ meson contribution to $P_\gamma(\sigma)$ and to $\omega_\sigma^\pi \approx 0.45$ for the pion fluctuations.

III. COLOR FLUCTUATIONS AND THE NUMBER OF WOUNDED NUCLEONS IN γA SCATTERING

In the case of the hadron–nucleus scattering, one can use the Glauber multiple scattering theory to calculate the distribution over the number of wounded nucleons [6]. This calculation can be generalized to the case of photon projectiles. Then, for the photon–nucleus cross section corresponding to exactly ν inelastic interactions with the target nucleons, σ_ν , one obtains in the high-energy optical model limit:

$$\sigma_\nu = \int d\sigma P_\gamma(\sigma) \binom{A}{\nu} \int d^2\vec{b} \left[\frac{\sigma_{in}(\sigma) T_A(b)}{A} \right]^\nu \left[1 - \frac{\sigma_{in}(\sigma) T_A(b)}{A} \right]^{A-\nu}, \quad (11)$$

where \vec{b} is the impact parameter; σ_{in} is the inelastic, non-diffractive cross section for the configuration characterized by the total cross section σ ; $T_A(b) = \int dz \rho_A(b, z)$ in the nuclear optical density, where $\rho_A(r)$ is the density of nucleons. Note that we use $\sigma_{in} = 0.85 \sigma$ and the Wood–Saxon density of nucleons for the ^{208}Pb target [9] in our analysis.

One of important advantages of the above equation is that unlike the standard Glauber model calculation [6], it accounts for inelastic diffractive processes in the intermediate states by including the contribution of the photon diffraction into large masses. A Monte-Carlo procedure to include finite size effects as well as short-range correlations between nucleons was developed in [9].

The probability to have exactly ν wounded nucleons in γA scattering, $P(\nu)$, reads:

$$P(\nu) = \frac{\sigma_\nu}{\sum_1^\infty \sigma_\nu}, \quad (12)$$

where σ_ν are given by Eq. (11). The probability distribution $P(\nu)$ calculated using Eqs. (11) and (12) is shown in Fig. 2 by the curve labeled “Color Fluctuations”. For comparison, we also show the results of the calculation, where the effect of CFs is neglected and the photon is represented by an effective fluctuation interacting with the total cross section $\sigma = 25$ mb; the corresponding curve is labeled “Glauber”.

Equation (11) does not take into account that in QCD, configurations corresponding to a small cross section of the interaction with the nucleon at high energies interact with the collective small- x gluon field of the nucleus, which is suppressed compared to the sum of the individual gluon fields of the nucleons due to the phenomenon of the leading twist (LT) nuclear shadowing [38]. This is supported by the observation of the large LT shadowing in coherent photoproduction of J/ψ in Pb-Pb UPCs at the LHC [39–41]. This implies that Eq. (11) underestimate the probability of the interaction with two and more nucleons for small σ , which is determined by the LT nuclear shadowing. To take into the account this effect, we modify Eq. (11) and use the following expression:

$$\sigma_\nu = \int_0^\infty d\sigma P_\gamma(\sigma) \binom{A}{\nu} \left[\frac{\sigma_{in}}{\sigma_{\text{eff}}} \Theta(\sigma_0 - \sigma) + \Theta(\sigma - \sigma_0) \right] \int d^2\vec{b} \left[\frac{\sigma_{\text{eff}}^{in} T_A(b)}{A} \right]^\nu \left[1 - \frac{\sigma_{\text{eff}}^{in} T_A(b)}{A} \right]^{A-\nu}, \quad (13)$$

where the suppression factor of $\sigma^{in}/\sigma_{\text{eff}}^{in} \approx \sigma/\sigma_{\text{eff}} < 1$ models the effect of the LT shadowing; $\sigma_{\text{eff}} = \sigma$ for $\sigma > \sigma_0$; $\sigma_0 = 20$ mb is the maximal cross section, where the LT shadowing is present (see below). For each $\sigma < \sigma_0$, the effective

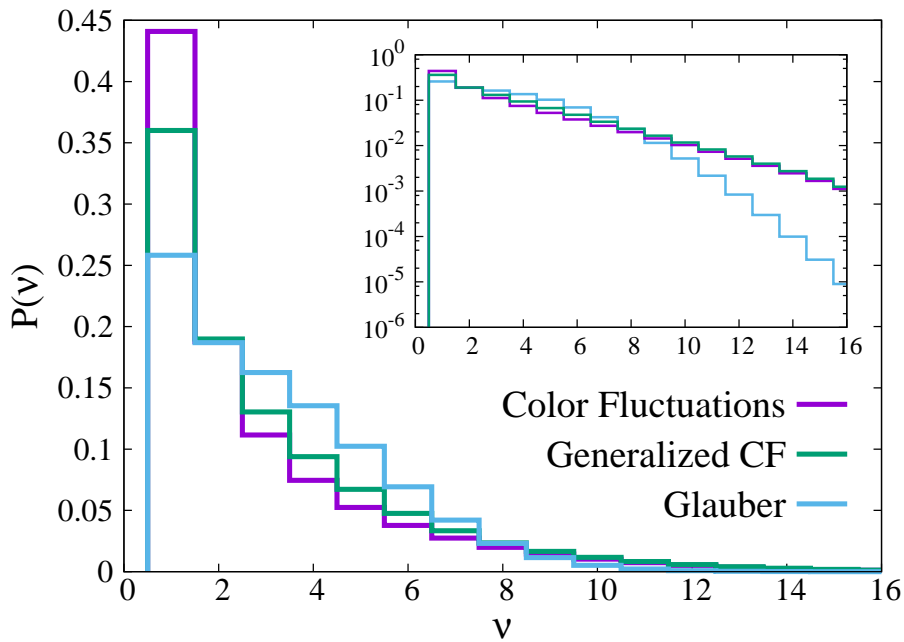


FIG. 2: The probability distributions $P(\nu)$ of the number of inelastic collisions ν . Predictions of Eqs. (11) and (13) are shown by the curves labeled “Color Fluctuations” and “Generalized CF”, respectively. For comparison, the Glauber model calculation with $\sigma = 25$ mb, which neglects the effect of CFs, is shown by the curve labeled “Glauber”.

cross section σ_{eff} is defined as the cross section corresponding to the gluon shadowing ratio $R_g(x)$ [38] calculated in the high-energy eikonal approximation:

$$R_g(x_{\text{eff}}, Q_{\text{eff}}^2) = \frac{xg_A(x_{\text{eff}}, Q_{\text{eff}}^2)}{Axg_N(x_{\text{eff}}, Q_{\text{eff}}^2)} = \frac{2}{A\sigma_{\text{eff}}} \int d^2\vec{b} \left(1 - e^{-\sigma_{\text{eff}}/2T_A(b)}\right), \quad (14)$$

where x_{eff} and Q_{eff}^2 are the light-cone momentum fraction and the resolution scale, respectively, which correspond to the dipole for the given cross section $\sigma = \sigma_{q\bar{q}}(W, d_t, m_q)$ (the transverse size d_t), see Eq. (5). This prescription for σ_{eff} is based on the observation that since the non-vector-meson component of $P_\gamma(\sigma)$ is relatively small, the gluon shadowing can be considered in a simplified approximation, where CFs for the interaction with $N \geq 2$ nucleons are small and, hence, R_g is given by a single effective rescattering cross section.

To estimate σ_0 , we notice that the factor of nuclear suppression of coherent J/ψ photoproduction on nuclei is described very well for the LT nuclear shadowing. In particular, $R_g \approx 0.6$ for $x = 10^{-3}$ [41], which according to Eq. (14) corresponds to $\sigma_{\text{eff}} = 17$ mb. Therefore, in our analysis we take $\sigma_0 = 20$ mb. A numerical analysis indicates that the results of our calculation depend weakly on the method of smooth interpolation in Eq. (9) and the assumption about the value of the ratio $\sigma^{\text{in}}/\sigma_{\text{eff}}^{\text{in}}$. The result of the calculation of the distribution over ν using Eq. (13) is shown in Fig. 2 by the curve labeled “Generalized CF”.

The results presented in Fig. 2 deserve a discussion. For one inelastic photon–nucleus interaction ($\nu = 1$), CFs in the photon lead to an almost a factor of two enhancement of $P(\nu)$ compared to the standard Glauber model prediction. Thus, an inclusion of the approximately 30% small- σ component of the photon wave function (see the discussion in the Introduction), leads to a large effect in the inelastic γA scattering. This effect is reduced approximately by a factor of two when include the LT nuclear shadowing (compare the “Color Fluctuations” and “Generalized CF” curves). As ν increases, the small- σ contribution to the distribution $P_\gamma(\sigma)$ becomes progressively less important and all three models give similar results for $2 < \nu < 8$, where the contribution of the two terms in the integrand of Eq. (13) approximately compensate each other. For large $\nu > 10$, the two models including the effect of CFs in the photon predict a much broader distribution $P(\nu)$ than the Glauber model; the enhancement at large ν comes from the contribution of the large-mass inelastic diffractive states implicitly included in Eqs. (11) and (13), which are absent in the Glauber model.

IV. COLOR FLUCTUATIONS AND THE DISTRIBUTION OVER TRANSVERSE ENERGY

It is impossible to directly measure the number of inelastic interactions ν for collisions with nuclei. However, the analysis of [5] suggests that the distribution over the total transverse energy, ΣE_T , near the nuclear fragmentation region ($-5 < \eta < -3$) is weakly influenced by energy conservation effects (due to the approximate Feynman scaling in this region), and is also weakly correlated with the activity in the rapidity-separated central and forward regions. This expectation is validated by a recent measurement of ΣE_T as a function of hard scattering kinematics in pp collisions at the LHC [42].

Due to the weak sensitivity to the projectile fragmentation region, we expect that the ΣE_T distributions in pA and γA scattering at similar energies should have similar shapes for the same ν . In Ref. [5], a model was developed for the distribution over ΣE_T as a function of ν , $f_\nu(\Sigma E_T)$, to describe the ΣE_T distribution for pA scattering at $-3.2 > \eta > -4.9$ and $\sqrt{s} = 5.02$ TeV. It is natural to expect in the spirit of the KNO scaling that the distribution over ΣE_T , when normalized to the average energy release in pp scattering, weakly depends on the incident collision energy. That is, the distribution over $y = \Sigma E_T / \langle \Sigma E_T(NN) \rangle$ has approximately the same shape at different energies. Hence we model the distribution over y for photon–nucleus collisions using $F_\nu(y) = \langle \Sigma E_T(NN) \rangle f_\nu(y)$, where the factor of $\langle \Sigma E_T(NN) \rangle$ is a Jacobian to keep normalization of $\int F_\nu(y) dy = P(\nu)$.

The results of the calculation are presented in Fig. 3 for the Generalized Color Fluctuations (GCF) model showing contributions of events with different ν to the normalized distribution over y . One can see that the distribution is predicted to be much broader than in the γp scattering. The results indicate that for $\Sigma E_T / \langle \Sigma E_T(NN) \rangle \leq 1$, the contribution of the interactions with one nucleon dominates. It will be possible to determine the distribution over y for ν from the γp data and to check that it is close to the y -distribution in the process of dijet production in the interaction of the direct photon ($x_\gamma = 1$) with a gluon with $x_A \geq 0.01$ for which $\nu = 1$. Hence it would be straightforward to determine the fraction of the $\nu = 1$ and $\nu > 1$ events which is quite sensitive to the model, see Fig. 2.

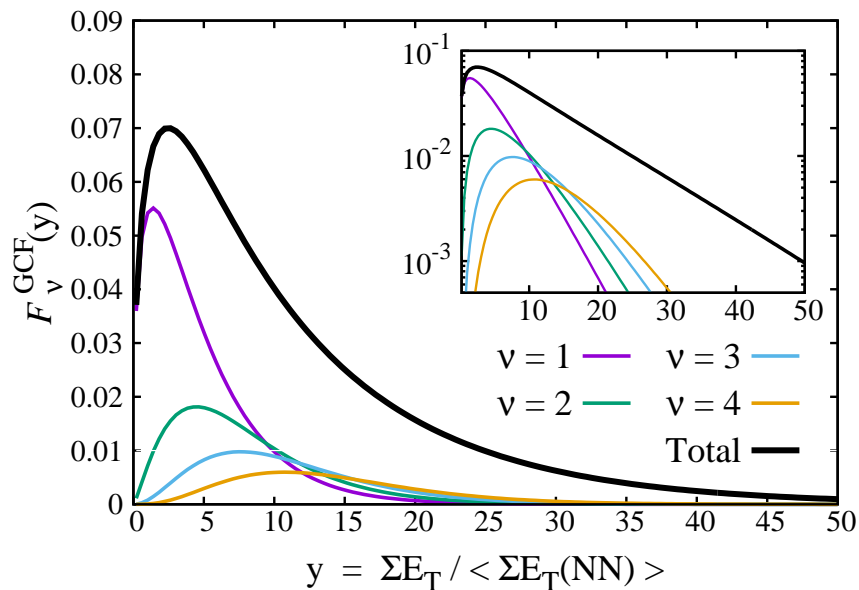


FIG. 3: The probability distributions over the transverse energy in the Generalized Color Fluctuations (GCF) model. The distributions are normalized to average transverse energy in pp collisions.

We also checked that smearing over y does not wipe out the difference between the models for the ν distribution, see Fig. 4.

Overall we observe that the y distribution is predicted to be much broader in γA collisions than in γp scattering. Thus by studying the distribution over ΣE_T for different forward triggers, it would be possible to determine the distribution over ν and use it to determine both $\langle \sigma \rangle$ and the variance of the $P_\gamma(\sigma)$ distribution for selected configuration. For example, in the color fluctuation model of Eq. (11) (*cf.* [9, 43]), which does not include the LT shadowing effects, one obtains the following relations for the average number of inelastic collisions $\langle \nu \rangle$,

$$\langle \nu \rangle = \frac{A\sigma_{in}(\gamma N)}{\sigma_{in}(\gamma A)}, \quad (15)$$

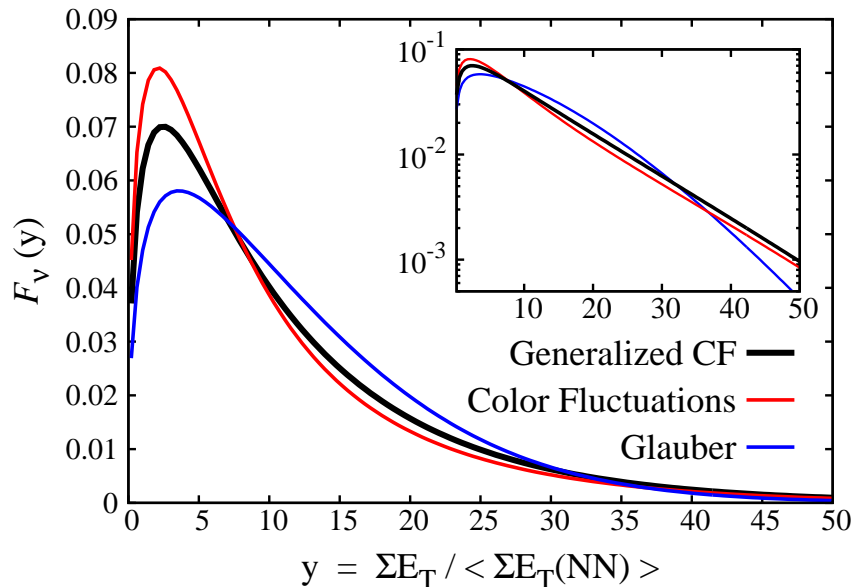


FIG. 4: The probability distributions over the transverse energy normalized to average transverse energy in pp collisions in different models.

and for the variance of the cross section for a specific trigger,

$$\frac{\langle \sigma_{trig}^2 \rangle}{\langle \sigma_{trig} \rangle} = \frac{\langle \nu^2 \rangle / \langle \nu \rangle - 1}{A-1} \frac{A^2}{\int d^2b T_A^2(b)}. \quad (16)$$

Obviously similar considerations are applicable for the γA interactions with a special trigger including jet production, production of charm, etc. In the case of forward dijet production, for direct photon for $x_A \leq 0.01$, the leading twist shadowing should set in resulting in a broader distribution over ν as compared to the interactions with $x_A > 0.01$ (corresponding to $\nu = 1$), see the discussion in sections 6.3 and 6.4 of [38]. For the resolved photons, the distribution over ν (and hence over ΣE_T) should become broader with a decrease of x_γ since hadronic configurations with smaller x_γ have a larger transverse size. One also expects that for sufficiently small $x_\gamma < 0.1$, the hard process would select generic configurations in the photon and, hence, the distribution over ΣE_T would approach the distribution for generic (without trigger) γA collisions. Note that first studies of diffractive dijet photoproduction in pp , pA and AA UPCs at the LHC in next-to-leading order (NLO) QCD, where CFs in the photon were used to model the effect of factorization breaking, were reported in [44].

In the case of production of leading charm, small-size dipoles dominate (the variation of the transverse size is regulated by m_c and $p_t(\text{charm})$), which allows one to study leading twist shadowing effects in the charm channel. For instance, for $x \sim 10^{-3}$, one expects $\langle \nu \rangle \sim 2$ and the corresponding reduction of $\sigma_{in}^{charm}(\gamma A)/A\sigma_{in}^{charm}(\gamma p)$, see Eq. (15).

V. CONCLUSIONS

In this paper, we quantify the general property of photon–hadron interactions at high energies that the photon can be viewed as a superposition of configurations interacting with different cross sections, which we call the phenomenon of color fluctuations (CFs), and propose a model for the distribution $P_\gamma(\sigma)$ describing these CFs. Using this model and also additionally taking into account the effect of leading twist nuclear shadowing for small- σ configurations, we for the first time give predictions for the distribution over the number of inelastic interactions ν in photon–nucleus scattering. Our results show that CFs lead to a dramatic enhancement of this distribution at the small $\nu = 1$ and the large $\nu > 10$ compared to the standard Glauber model calculations. We also study the effect of CFs on the total transverse energy ΣE_T released in inelastic γA scattering with different triggers and point to specific indications of the CF effect. Our predictions can be tested in the photon–nucleus (γA) interactions in UPCs of ions at the LHC,

which are characterized by high-intensity fluxes of quasi-real photons in a wide energy spectrum and which can be viewed as an effective “strengthenometer” of the different components of the photon wave function.

It would also allow one to obtain (using central tracking of the LHC detectors) unique information on the centrality dependence of the production of forward hadrons carrying a large fraction of the photon momentum ($x_F \geq 0.5$). For soft interactions, experiments at fixed-target energies did indicate a strong suppression of the low- p_t and large- x_F hadron production. At the same time, very little experimental information is available on suppression of the leading hadron production at the collider energies and on its W dependence. These and other related topics will be discussed in more detail elsewhere.

Acknowledgments

L.F.’s and M.S.’s research was supported by the US Department of Energy Office of Science, Office of Nuclear Physics under Award No. DE-FG02-93ER40771.

-
- [1] T. H. Bauer, *et al.*, *Rev. Mod. Phys.* **50**, 261 (1978) [Erratum-ibid. **51**, 407 (1979)].
- [2] L. L. Frankfurt, G. A. Miller and M. Strikman, *Ann. Rev. Nucl. Part. Sci.* **44**, 501 (1994) [hep-ph/9407274].
- [3] L. Frankfurt, V. Guzey and M. Strikman, *J. Phys. G* **27**, R23 (2001) [hep-ph/0010248].
- [4] D. Dutta, K. Hafidi and M. Strikman, *Prog. Part. Nucl. Phys.* **69**, 1 (2013) [arXiv:1211.2826 [nucl-th]].
- [5] G. Aad *et al.* [ATLAS Collaboration], *Eur. Phys. J. C* **76**, no. 4, 199 (2016) [arXiv:1508.00848 [hep-ex]].
- [6] L. Bertocchi and D. Treleani, *J. Phys. G* **3**, 147 (1977).
- [7] G. Baym, B. Blattel, L. L. Frankfurt, H. Heiselberg and M. Strikman, *Phys. Rev. C* **52**, 1604 (1995) [nucl-th/9502038].
- [8] V. Guzey and M. Strikman, *Phys. Lett. B* **633**, 245 (2006) [*Phys. Lett. B* **663**, 456 (2008)] [hep-ph/0505088].
- [9] M. Alvioli and M. Strikman, *Phys. Lett. B* **722**, 347 (2013) [arXiv:1301.0728 [hep-ph]].
- [10] G. Aad *et al.* [ATLAS Collaboration], *Phys. Lett. B* **748**, 392 (2015) [arXiv:1412.4092 [hep-ex]].
- [11] S. Chatrchyan *et al.* [CMS Collaboration], *Eur. Phys. J. C* **74**, no. 7, 2951 (2014) [arXiv:1401.4433 [nucl-ex]].
- [12] A. Adare *et al.* [PHENIX Collaboration], *Phys. Rev. Lett.* **116**, no. 12, 122301 (2016) [arXiv:1509.04657 [nucl-ex]].
- [13] M. Alvioli, B. A. Cole, L. Frankfurt, D. V. Perepelitsa and M. Strikman, *Phys. Rev. C* **93**, no. 1, 011902 (2016) [arXiv:1409.7381 [hep-ph]].
- [14] J. Adam *et al.* [ALICE Collaboration], *JHEP* **1509**, 095 (2015) [arXiv:1503.09177 [nucl-ex]].
- [15] L. Frankfurt, V. Guzey, M. Strikman and M. Zhalov, *Phys. Lett. B* **752**, 51 (2016) [arXiv:1506.07150 [hep-ph]].
- [16] A. J. Baltz *et al.*, *Phys. Rept.* **458**, 1 (2008) [arXiv:0706.3356 [nucl-ex]].
- [17] A. Accardi *et al.*, arXiv:1212.1701 [nucl-ex].
- [18] D. Boer *et al.*, arXiv:1108.1713 [nucl-th].
- [19] V. Guzey, M. Strikman and M. Zhalov, *Eur. Phys. J. C* **74**, no. 7, 2942 (2014) [arXiv:1312.6486 [hep-ph]].
- [20] V. N. Gribov, *Sov. Phys. JETP* **30**, 709 (1970) [*Zh. Eksp. Teor. Fiz.* **57**, 1306 (1969)].
- [21] J. J. Sakurai, *Annals Phys.* **11**, 1 (1960).
- [22] R. P. Feynman, *Photon-hadron interactions*, (Benjamin, Reading 1972), 282 p.
- [23] J. D. Bjorken, *Conf. Proc. C* **710823**, 281 (1971).
- [24] L. L. Frankfurt and M. I. Strikman, *Phys. Rept.* **160**, 235 (1988).
- [25] M. L. Good and W. D. Walker, *Phys. Rev.* **120**, 1857 (1960).
- [26] H. I. Miettinen and J. Pumplin, *Phys. Rev. D* **18**, 1696 (1978).
- [27] B. Z. Kopeliovich, L. I. Lapidus and A. B. Zamolodchikov, *JETP Lett.* **33**, 595 (1981).
- [28] D. R. Harrington, *Phys. Rev. C* **52**, 926 (1995) [nucl-th/9503006].
- [29] B. Blaettel, *et al.*, *Phys. Rev. D* **47**, 2761 (1993).
- [30] L. Frankfurt, V. Guzey and M. Strikman, *Phys. Rev. D* **58**, 094039 (1998) [hep-ph/9712339].
- [31] L. Frankfurt, A. Radyushkin and M. Strikman, *Phys. Rev. D* **55**, 98 (1997) [hep-ph/9610274].
- [32] B. Blaettel, G. Baym, L. L. Frankfurt and M. Strikman, *Phys. Rev. Lett.* **70**, 896 (1993); L. Frankfurt, G. A. Miller and M. Strikman, *Phys. Lett. B* **304**, 1 (1993).
- [33] N. N. Nikolaev and B. G. Zakharov, *Z. Phys. C* **49**, 607 (1991).
- [34] M. McDermott, L. Frankfurt, V. Guzey and M. Strikman, *Eur. Phys. J. C* **16**, 641 (2000) [hep-ph/9912547].
- [35] L. Frankfurt, M. McDermott and M. Strikman, *JHEP* **0103**, 045 (2001) [hep-ph/0009086].
- [36] K. A. Olive *et al.* [Particle Data Group Collaboration], *Chin. Phys. C* **38**, 090001 (2014).
- [37] T. J. Chapin *et al.*, *Phys. Rev. D* **31**, 17 (1985).
- [38] L. Frankfurt, V. Guzey and M. Strikman, *Phys. Rept.* **512**, 255 (2012) [arXiv:1106.2091 [hep-ph]].
- [39] B. Abelev *et al.* [ALICE Collaboration], *Phys. Lett. B* **718**, 1273 (2013) [arXiv:1209.3715 [nucl-ex]].
- [40] E. Abbas *et al.* [ALICE Collaboration], *Eur. Phys. J. C* **73**, no. 11, 2617 (2013) [arXiv:1305.1467 [nucl-ex]].
- [41] V. Guzey, E. Kryshen, M. Strikman and M. Zhalov, *Phys. Lett. B* **726**, 290 (2013) [arXiv:1305.1724 [hep-ph]].
- [42] G. Aad *et al.* [ATLAS Collaboration], *Phys. Lett. B* **756**, 10 (2016) [arXiv:1512.00197 [hep-ex]].

- [43] M. Alvioli, L. Frankfurt, V. Guzey and M. Strikman, *Phys. Rev. C* **90**, 034914 (2014) [arXiv:1402.2868 [hep-ph]].
- [44] V. Guzey and M. Klasen, *JHEP* **1604**, 158 (2016) [arXiv:1603.06055 [hep-ph]].